



Characterization and modeling of manganese effect on strength and strain hardening of martensitic carbon steels

Artem Arlazarov, Olivier Bouaziz, Alain Hazotte, Mohamed Gouné, Sébastien Allain

► To cite this version:

Artem Arlazarov, Olivier Bouaziz, Alain Hazotte, Mohamed Gouné, Sébastien Allain. Characterization and modeling of manganese effect on strength and strain hardening of martensitic carbon steels. ISIJ international, 2013, 53 (6), pp.1076-1080. 10.2355/isijinternational.53.1076 . hal-00845143

HAL Id: hal-00845143

<https://hal.science/hal-00845143>

Submitted on 1 Aug 2018

HAL is a multi-disciplinary open access archive for the deposit and dissemination of scientific research documents, whether they are published or not. The documents may come from teaching and research institutions in France or abroad, or from public or private research centers.

L'archive ouverte pluridisciplinaire **HAL**, est destinée au dépôt et à la diffusion de documents scientifiques de niveau recherche, publiés ou non, émanant des établissements d'enseignement et de recherche français ou étrangers, des laboratoires publics ou privés.

Characterization and Modeling of Manganese Effect on Strength and Strain Hardening of Martensitic Carbon Steels

Artem ARLAZAROV,^{1,3)*} Olivier BOUAZIZ,^{1,2)} Alain HAZOTTE,³⁾ Mohamed GOUNÉ⁴⁾ and Sébastien ALLAIN¹⁾

1) ArcelorMittal Global Research and Development, Voie Romaine-BP30320, 57283 Maizières-lès-Metz Cedex France.

2) Centre des Matériaux, Ecole des Mines de Paris, CNRS UMR 7633, B.P. 87, 91003 Evry Cedex, France. 3) Laboratoire d'Etude des Microstructures et de Mécanique des Matériaux (LEM3), CNRS UMR 7239, Université de Lorraine, 57012 Metz Cedex, France. 4) Institut de Chimie de la Matière Condensée de Bordeaux (ICMCB), CNRS UPR 9048, 87 avenue du Docteur Schweitzer, 33609 Pessac, France.

(Received on December 12, 2012; accepted on March 11, 2013)

Carbon and manganese combined effect on the mechanical behavior of martensite was characterized and analyzed using literature and new experimental data of various carbon-manganese steels. A synergy effect of carbon and manganese on the martenstite strength and strain hardening was detected and was then taken into account in a specific way in the simplified model, based on a Continuous Composite Approach. Model was adjusted with only one fitting parameter and the obtained results are in good agreement with experimental stress-strain curves.

KEY WORDS: martensite; carbon; medium Mn; strain-hardening; modeling.

1. Introduction

Martensite is one of the hardest phases in the steel and also one of the most complex due to its “natural” nanostructure. Development of almost all very high strength steels for automotive or industry market is hardly possible without use of this constituent. Dual-Phase steel is a common example of martensite use, when its strength is combined with the ductility of ferrite to offer a large range of strength-ductility balances for different applications. A lot of studies concerning martensite structure and strength are already done and the obtained scientific knowledge is synthesized in form of reviews.^{1,2)}

Mechanical behavior of martensitic steel seems to be mainly controlled by one major factor – its initial carbon content. The evolution of martensite hardness related to its carbon content²⁾ is probably the most generally acknowledged correlation between a mechanical and a metallurgical parameter. Influence of other microstructural characteristics like sizes of laths, packets or prior austenite grains is still widely discussed in the literature.^{3–5)}

Surprisingly, the amount of considerations in the literature about strain-hardening mechanisms of martensitic steels is quite low, probably related to their poor uniform elongation (*i.e.* necking strain). Principally, the mechanical behavior of martensite is described either with phenomenological polynomial law⁶⁾ or it is reduced to an elastic or an elastic-perfectly plastic law.⁷⁾ However, recently a Continuum Composite Approach (CCA) was proposed to predict the

complete tensile curves of as-quenched martensitic steels.⁸⁾ The general idea of this approach is to consider martensite as a composite of elastic-perfectly plastic phases in interaction. All the phases have the same Young modulus, and the density of probability to find a phase with a given yield strength defines the so-called “stress spectrum”. This permits to describe the tensile behavior of martensite in a univocal way.

Although, there is an important quantity of data about different alloying elements influence on the martensite hardness,^{9,10)} a few data are found about the substitutional elements influence on the strain hardening of martensitic steels.¹¹⁾ In the present work, Mn effect on the strain hardening of martensitic steels is characterized. Based on CCA a simplified model to describe the mechanical behavior of martensite is proposed and a special manner to introduce the influence of Mn addition is suggested.

2. Experimental Procedure

Four steels with different combinations of carbon (C) and manganese (Mn) contents were prepared using vacuum induction melting. The chemical compositions of these steels, as well as of some selected C–Mn steels from previously published studies are shown in Table 1. The slabs were hot rolled, and then cold rolled to 1.2 mm thickness. Cold rolled specimens were austenitized 10°C above Ac_3 temperature (the temperature is indicated in Table 1) for 30 minutes, and then water quenched (~1000°C/s). For each steel two tensile tests at a constant strain rate of 0.008 s⁻¹ were performed on the samples with gauge length 50 mm and width 12.5 mm, according to the ISO procedure. Table

* Corresponding author: E-mail: artem.arlazarov@arcelormittal.com
DOI: <http://dx.doi.org/10.2355/isijinternational.53.1076>

2 shows the measured tensile properties of studied steels.

To confirm the martensitic state of two medium Mn (4.7 wt.%) steels, the microstructure of quenched samples was investigated using optical microscope and X-ray diffraction. So-called Dino etching was used to reveal the microstructure. Dino etchant was prepared from the following chemical compounds: 140 ml of distilled water, 100 ml of hydrogen peroxide (H_2O_2 30%), 4 g of ethane diacid ($C_2H_2O_4$ – $2H_2O$), 2 ml of sulphuric acid (H_2SO_4) and 1.5 ml fluohydric acid (HF). The applications of Dino reagent are miscellaneous. Generally, it can be used to reveal different microstructure constituents and in some cases their boundaries. In our case it was utilized in order to reveal martensitic microstructure and to verify if any ferrite was formed during cooling. **Figure 1** shows the outcomes of this analysis. Figures 1(a) and

1(b) present a typical lath martensite structure with the revealed prior austenite grain boundaries, also the absence of ferrite was confirmed. X-ray diffraction (XRD) with Co $K\alpha$ radiation was applied in order to reveal the presence of

Table 2. Measured mechanical properties of studied steels: yield strength ($YS_{0.2}$), ultimate tensile strength (UTS), uniform (Uel) and total (TE) elongation, respectively.

Ref.	$YS_{0.2}$ [MPa]	UTS [MPa]	Uel [%]	TE [%]
0.3C	1 333	1 875	3.3	4.6
0.36C	1 439	2 150	4.0	6.3
0.1C–5Mn	1 049	1 387	3.0	5.2
0.15C–5Mn	1 258	1 663	3.7	3.7

Table 1. Chemical composition of studied and previously published steels (wt.%), holding temperature for the studied steels and corresponding references. For each steel first column gives the reference (Steel) that will be used further in the article.

Steel	Composition (wt.%)					T_{hold} ($^{\circ}C$) ($Ac_3+10^{\circ}C$)	Source
	C	Mn	Si	Cr	Ti		
0.3C	0.29	1.20	0.25	0.17	0.04	850	This study
0.36C	0.36	1.22	0.23	0.10	0.04	830	This study
0.1C–5Mn	0.10	4.74	—	—	—	760	This study
0.15C–5Mn	0.15	4.73	—	—	—	750	This study
0.01C–3Mn	0.01	2.92	0.01	0.11	0.04		Zhu <i>et al.</i> ¹²⁾
0.09C	0.09	1.90	0.15	0.10	—		Allain <i>et al.</i> ⁸⁾
0.15C	0.15	1.90	0.22	0.20	—		Pushkareva I. ¹³⁾
0.22C	0.22	1.18	0.27	0.21	—		Allain <i>et al.</i> ⁸⁾

“—” means less than 0.01 wt.% for Si and Cr and less than 0.001 wt.% for Ti.

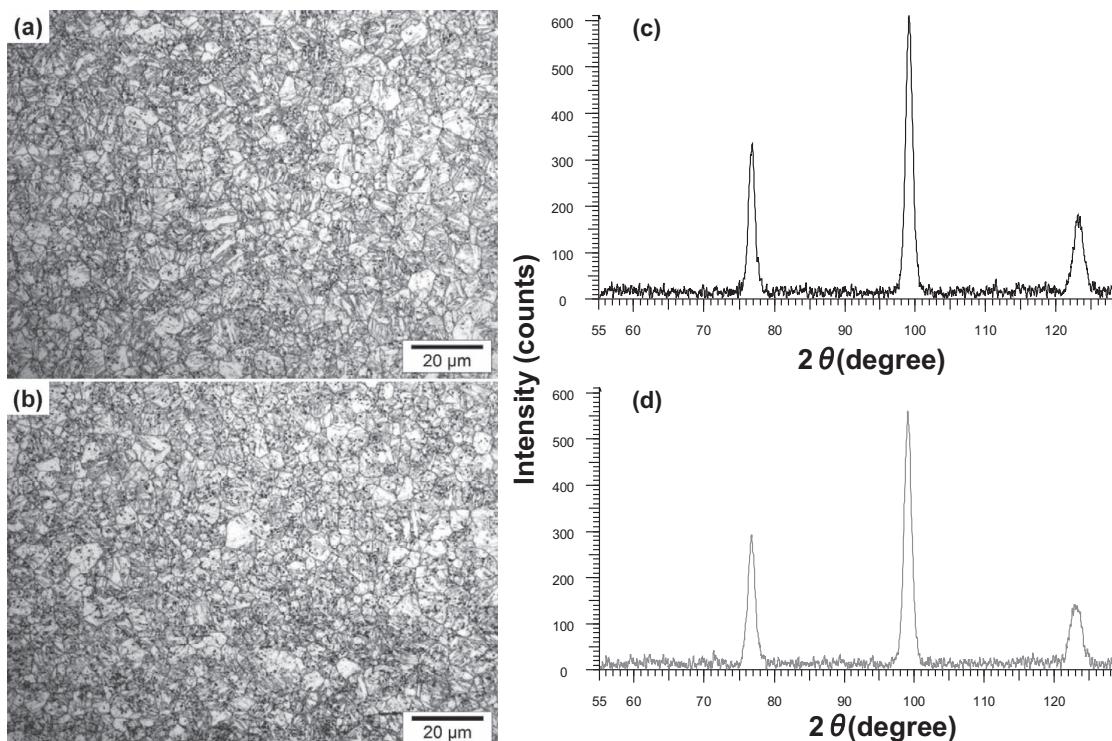


Fig. 1. (a) and (b) are the microstructures of two medium Mn steels revealed with Dino etching and observed with optical microscope, (c) and (d) are their respective X-ray spectra: (a) and (c) – 0.1C–5Mn, (b) and (d) – 0.15C–5Mn.

retained austenite. The X-ray spectra (Figs. 1(c) and 1(d)) demonstrate only ferritic peaks: $(220)_{\alpha}$, $(211)_{\alpha}$ and $(200)_{\alpha}$. Hence it is concluded that the structure is fully martensitic.

3. Results and Discussion

Figure 2 presents the results of experimental tensile tests performed in the present study along with the results collected from the previous works.^{8,12,13)} The true stress evolution as a function of true strain is shown in Fig. 2(a), meanwhile Fig. 2(b) shows the related strain hardening rate evolution as a function of true stress (so-called Kocks-Mecking plot^{14,15)}). For all studied martensitic steels some general highlights can be stated:

- Conventional yield stress seems to be a function of martensite carbon and manganese contents.
- High work-hardening rate is observed and it increases up to necking strain in accordance with the carbon and manganese contents.

From Fig. 2(a) it can be seen that the true stress-true strain curve of 0.1C–5Mn is almost the same as for 0.15C, and that the true stress-true strain curve of 0.15C–5Mn is in between the curves of 0.22C and 0.3C. The same conclusion can be deduced from Fig. 2(b) which demonstrates the strain hardening evolution. The solid solution hardening of Mn cannot explain this difference in the behavior of martensitic steels

with high Mn content. Modification of solid solution hardening only shifts the curves to higher stress levels, but in the case of medium Mn steels a clear change in strain hardening of martensite can be found. According to F.B. Pickering and T. Gladman¹⁶⁾ the solid solution hardening of Mn can be evaluated using following relation: $S_{\text{Mn}} * \text{Mn wt.\%}$, where $S_{\text{Mn}} = 32$. This means that each percent of Mn increases strength on 32 MPa and for 4.7 wt.% of Mn the strength should increase on about 150 MPa. Figure 2(c) shows the experimental curves of 0.15C and 0.15C–5Mn, but also 0.15C curve shifted up at 150 MPa. This figure proves that such shift is not sufficient to match with 0.15C–5Mn; there are still about 125 MPa missing. But also the strain hardening rate, which is depicted in Fig. 2(b) is not the same. Thus it is considered that simple solid solution hardening cannot explain the behavior of martensite with medium content of Mn. It can be also observed from the Figs. 2(a) and 2(b) that the influence of Mn on stress and on strain hardening in the case of small carbon content (0.01C–3Mn) is rather limited. All these facts suggest that Mn content influences the martensite strength and strain hardening in obvious synergy with the carbon content of martensite.

Based on the CCA approach,⁸⁾ a simplified behavior law for martensitic steels is proposed. In order to describe the stress-strain curve of martensite as a large elasto-plastic transition the strain hardening can be expressed as the prod-

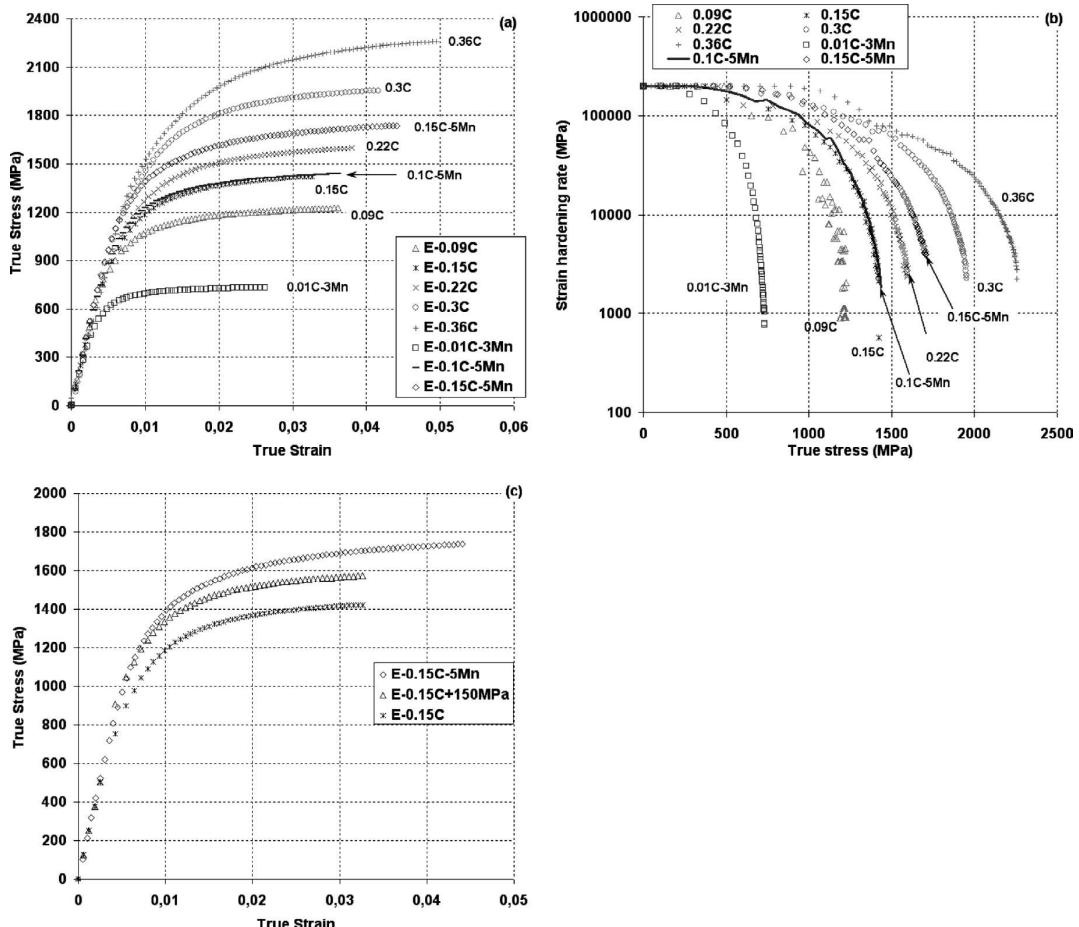


Fig. 2. (a) Experimental true stress-true strain curves of all studied martensitic steels; (b) the strain hardening rate as a true stress function of corresponding tensile tests presented in (a); (c) comparison of true stress-true strain curves of 0.15C and 0.15C–5Mn steels, and also the curve of 0.15C shifted up at 150 MPa, which corresponds to solid solution hardening of Mn.

uct of Young modulus (E) by the fraction of elastic zones ($1 - F$):

$$\frac{d\sigma}{d\varepsilon} = (1-F) \cdot E \quad \dots \dots \dots \quad (1)$$

where σ and ε are respectively the macroscopic stress and strain of the material.

The plasticized zones fraction F is chosen as a logistic law:

$$F = 1 - \exp\left(-\left(\frac{\sigma - \sigma_{\min}}{\sigma_0}\right)^p\right) \dots \quad (2)$$

where σ_{\min} is the minimum stress necessary to start to plasticize and, p and σ_0 are the parameters that control the shape of $F(\sigma)$ curve (Fig. 3(a)). In the first stage of tensile test, the macroscopic stress is lower than the elastic threshold ($\sigma < \sigma_{\min}$), hence $F = 0$ and the material exhibits completely elastic behavior. When the applied stress (σ) became more important than σ_{\min} , then F starts to increase, meaning that the plasticized zones fraction increases.

Model adjustment with the experimental and literature data shows that σ_{\min} and p can be taken as constants for all considered steels, and the following values are found to be

optimal: $\sigma_{\min} = 450$ MPa and $p = 2.5$. Thus, only one variable parameter, σ_0 , is used to obtain the best fitting results between model and experiments. It is found that both C and Mn have an important influence on σ_0 . A linear dependence between σ_0 and C_{eq} is established in the form of subsequent equation:

$$\sigma_0 = 130 + 1997 \cdot C_{ea} \quad \dots \dots \dots \quad (3)$$

where C_{eq} is the parameter that considers the concomitant influence of C and Mn . It is proposed to take into account this synergy of C and Mn in the following way:

$$C_{eq} = C \cdot \left(1 + \frac{Mn}{K_{Mn}} \right) \dots \dots \dots \quad (4)$$

where C and Mn represent initial C and Mn (wt.%) contents, and K_{Mn} is the coefficient of the Mn influence. Finally, from the collected experimental data (Tables 1, 2 and Fig. 2) it is possible to find the optimum value for $K_{Mn} = 3.5$.

The σ_0 evolution with C_{eq} is shown in Fig. 3(b): experimentally adjusted points are compared to the ones predicted with Eq. (3).

The final results of the model are presented and compared to the experimental data in Fig. 4. The results of stress-strain curves prediction are separated into two graphs (Figs. 4(a) and 4(b)) to have a better vision of medium Mn steels curves. As it can be seen, this simple model accurately predicts the whole stress-strain curves of different martensitic steels with varied C and Mn contents. On the other hand, it can be noticed that the simulated curves are not perfect and there are some mismatches. However, the maximum difference between model and experimental curves in terms of stress is less than 60 MPa and this represent less than 5% of the maximum flow stress.

Figures 4(c) and 4(d) present the evolution of strain hardening rate as a function of stress and as a function of strain, respectively. Taking into account that modeling of derivative is more complex than modeling of a function itself; the proposed model gives very satisfactory results of strain hardening rate evolution. These figures also shows that the model accounts well the synergy influence of C and Mn on the strain hardening rate evolution.

Even though the results are satisfactory, it is evident that the proposed model is a simplified version of CCA published previously,⁸⁾ hence the global description of stress-strain curves is less precise, especially elasto-plastic transition. This can be clearly seen on the stress-strain curves of 0.22C, 0.15C and in particular 0.01C–3Mn steels. The discrepancy of the model is also related to the fact that only one fitting parameter is considered. This is done deliberately in order to simplify the understanding of the observed phenomenon of C–Mn synergy. Model response can be easily improved by relaxing the constraints on σ_{\min} making it variable and not constant. Nevertheless, to obtain good correlation between σ_{\min} and some metallurgical or microstructural parameters more data and studies are needed.

Future works are also necessary to understand physical mechanism of this C–Mn synergy and its relation with the microstructure. The outputs of these further investigations will be probably very helpful for further model improvement.

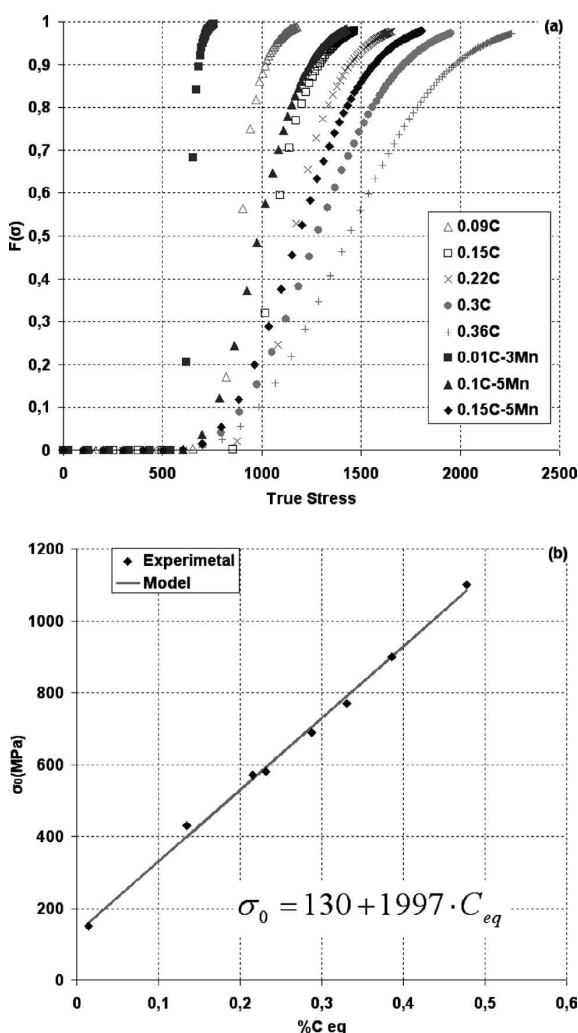


Fig. 3. (a) Evolution of modeled $F(\sigma)$ with the true stress; (b) Comparison of the σ_0 values: predicted with Eq. (3) (model) and experimentally adjusted ones.

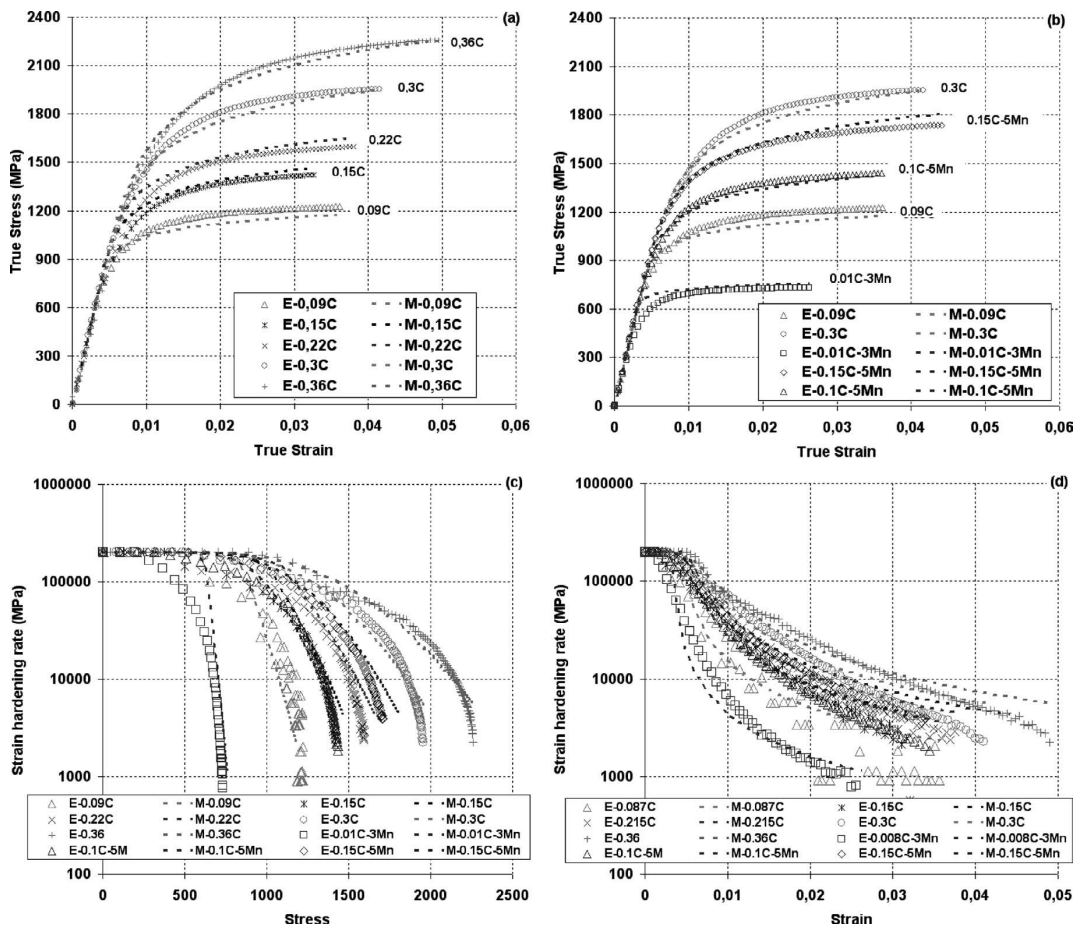


Fig. 4. Comparison of the model and experimental results. (a) and (b) show the stress-strain curves: (a) – steels with varied C content; (b) – steels with higher Mn content and two steels with standard (for AHSS) Mn content for comparison. (c) – evolution of strain hardening rate as a function of stress. (d) – evolution of strain hardening rate as a function of strain. “E” means experimental data and “M” means data from the model.

4. Conclusions

Mechanical behavior of martensite was studied using literature and new experimental data obtained on two medium carbon and two medium manganese steels. It was found that manganese increases strength and strain hardening of martensite in synergy with its carbon content. This synergy between carbon and manganese was taken into account in a specific way and the coefficient of the manganese influence was adjusted. More pragmatic model to describe mechanical response of martensitic steels was proposed based on Continuous Composite Approach developed previously. The results of adjusted model with only one fitting parameter showed very satisfactory agreement with the experimental data.

As the understanding of physical mechanism explaining the reported synergy between manganese and carbon on the behavior of martensite is not available, future investigations are planned in order to link the macroscopic martensite behavior and the related microstructure in presence of carbon and manganese.

Acknowledgements

The authors wish to express their gratitude to J. D. Puerta Velasquez from ARCELORMITTAL for sharing his knowledge and experimental results.

The authors are also grateful to D. Bouleau and J. Drillet from ARCELORMITTAL for their important contribution in the development of the metallographic etchings.

REFERENCES

- 1) G. B. Olson and W. S. Owen: Martensite, A tribute to Morris Cohen, ASM International, OH, (1992).
- 2) G. Krauss: *Mater. Sci. Eng.*, **A273–275** (1999), 40.
- 3) M. J. Roberts: *Metall. Trans.*, **1** (1970), 3287.
- 4) M. Kehoe and P. M. Kelly: *Scr. Metall.*, **4** (1970), 473.
- 5) S. Morito, H. Yoshida, T. Maki and X. Huang: *Mater. Sci. Eng.*, **A438–440** (2006), 237.
- 6) K. S. Choi, W. N. Liu, X. Sun and M. A. Khaleel: *Metall. Mater. Trans. A*, **40A** (2009), 796.
- 7) M. Delincé, Y. Bréchet, J. D. Embury, M. G. D. Geers, P. J. Jacques and T. Pardoen: *Acta Mater.*, **55** (2007), 2337.
- 8) S. Allain, O. Bouaziz and M. Takahashi: *ISIJ Int.*, **52** (2012), No. 4, 717.
- 9) R. A. Grange, C. R. Hribal and L. F. Porter: *Metall. Trans.*, **8A** (1977), 1775.
- 10) N. Yuriko, M. Okumura, T. Kasuya and H. J. U. Cotton: *Met. Constr.*, **19** (1987), No. 4, 217R.
- 11) A. G. Vasil'eva, D. A. Prokoshkin and V. V. Goryushin: *Met. Sci. Heat Treat.*, **16** (1974), No. 6, 507.
- 12) K. Zhu, O. Bouaziz, C. Oberbillig and M. Huang: *Mater. Sci. Eng.*, **A527** (2010), 6614.
- 13) I. Pushkareva: Ph.D report, INPL, (2009), http://pegase.scd.inpl-nancy.fr/theses/2009_PUSHKAREVA_I.pdf.
- 14) U. F. Kocks and H. Mecking: *Prog. Mater. Sci.*, **48** (2003), 171.
- 15) H. Mecking and U. F. Kocks: *Acta Metall.*, **29** (1981), 1865.
- 16) F. B. Pickering and T. Gladman: Metallurgical Developments in Carbon Steels, Iron and Steel Institute, Special Report, No. 81, London, (1963), 10.